

SOLAR DIAMETER MEASUREMENTS, A NEW APPROACH

J. ROSCH and R. YERLE

Pic du Midi and Toulouse Observatories.

The experiment we would like to present was originally intended, in the early seventies, to confirm - or not - by a completely different observing method, the solar oblateness announced by DICKE (1967) - a 0.1" difference between equatorial and polar diameters. This result has raised well known arguments, both experimental and astrophysical, the latter mostly related to the problem of a fast rotating core inside the sun. It appeared, afterwards, that various relativistic tests at least did not confirm the Brans-Dicke cosmology. Therefore, if an oblateness does exist, what about the secular advance of the perihelion of Mercury, etc..? Thus, it seemed worth to pursue our program.

Then, H.A. HILL and co-workers (1975) announced that they had found, in a different way, the solar oblateness to be consistent with the 27-day rotation of the outer layers, but the solar diameter to oscillate at a number of discrete frequencies; later on, HILL (1976) suggested that they could mean, rather oscillations in temperature, and developed with his associates, (HILL et al., 1979), the interpretation by fluctuations in the brightness distribution around the limb.

On another hand, it seems that more and more interest is taken, now, in the solar diameter in itself, leading to its possible secular changes. Therefore, a physical definition of what does "solar diameter" mean is needed, and the results below show the way to a measure of such a diameter, which could provide, in a second step, an absolute value.

Moreover, we shall see that an unexpected result already emerges from our preliminary observations, possibly bringing a new point into the problem of solar oscillations.

The main drawback of Dicke's as well as Hill's method is that they measure integrals of the flux around or across the limb (with a weighting in the second one)

and do not, therefore, discriminate directly between temperature and diameter changes. The approach we had in mind from the beginning was to have a differential definition of the limb, and then to detect, separately, through an integral, possible temperature changes.

The most obvious differential definition of the limb is as the point where the brightness gradient along a solar radius is maximum. But, then, two questions need to be answered : first, to which extent is the limb defined in that way independent from a temperature change ? And second, how to manage with the classical effect of the atmospheric spreading function upon the position of the inflexion point of the profile ?

For the first question, the simplest idea is to take a model of the solar atmosphere and compute the position of the maximum gradient on the resulting limb profile; then introduce various changes in the distribution of temperature versus altitude and compare the positions of the maximum gradient. HILL et al. (1975), in their first treatment of the problem of the solar diameter, used a model, based on the Stratoscope observations (ROGERSON, 1959), where they assumed a "vertical" drop of brightness down to zero at a position which, of course, they take as the very limb. In a more recent paper (HILL et al, 1978) they compute, through a theoretical model, the effect of non-adiabatic oscillations on the appearance of the limb, which, again, shows an onset of brightness from zero to a finite value at the very origin of the radial coordinate. We preferred to start with the classical HSRA model (Fig. 1) established upon a bulk of data collected in various spectral ranges, leading to a steep (but not vertical) drop of the limb brightness to a non-zero minimum, which one cannot forget when dealing with observational problems (^X).

Thanks to a program kindly provided by S. DUMONT, and dividing the solar atmosphere into 95 layers, 20 km thick in average, we could compute the position of the maximum gradient of the limb, first for the initial temperature vs height

(^X) Refinements to HSRA suggested by VERNAZZA et al. (1980) introduce only moderate shifts in the position and value of the temperature minimum, but do not change appreciably the shape of the temperature vs altitude distribution, and would not modify our conclusions.

distribution (Fig. 2), and then with various modifications as follows (the layers are numbered 1 to 95 inward, see Fig. 1) :

- a : constant ΔT for all layers;
- b_1, b_2, b_3 : constant ΔT in the outer (1-30), middle (31-65), or inner (65-95) slices;
- c_1, c_2 : 0 to $\pm \Delta T$, proportional to the altitude, from layer 95 to layer 1.

The results (Table 1) show that :

- 1) The drift is proportional to ΔT , the temperature difference, and does not exceed a few milliseconds of arc for temperature changes of the order of magnitude which is likely to occur; it will anyhow be possible to apply a small correction in position if, by measurements of another type, temperature differences are detected.
- 2) Only changes in the "middle" slice do result in a drift; this is not surprising, since only that one is effective in producing the limb profile;
- 3) A significant change in the value of the maximum logarithmic gradient appears as a function of temperature differences; this is a very important fact which will be taken into account later on in this paper.

Thus, we can conclude that the definition of the solar diameter by the distance between the inflexion points of opposite limb profiles has a definite geometrical value, since it does not depend upon possible temperature variations in the layers involved. Moreover, measuring directly the distance has the advantage of separating the variables diameter and temperature.

Now, about the observational problems. The main concern is the fact that the convolution of a uniformly bright half plane by a spreading function having a center of symmetry gives a profile with its inflexion point exactly on the geometrical edge of the object. If the object has a limb-darkening, the inflexion point is shifted inward by an amount δ increasing with the width of the spreading function. HILL et al (1975) computing this effect for a simplified model of the solar limb and for gaussian spreading functions of increasing widths, concluded, also from unsuccessful observations, that the method was hopeless.

Taking into account the angular resolution we are used to experience at Pic-du-Midi with our 50 cm refractor, we thought, from our part, that it was worth to be developed, and we tried to demonstrate it by a preliminary series of observations on one limb only.

Fig. 3 shows CRO tracings of the signal and of its first derivative during a scan across the limb. The scan, produced by a rotating glass cube, is very fast

($\approx 3000''$ per sec.) and this is fundamental to freeze the image; the scanning aperture is quite small ($0''1 \times 0''1$); the signal is sampled and stored for further computation of three quantities : the maximum slope \underline{m} , the abscissa \underline{x} of the point where the slope is maximum, taking as origin the edge of the window which limits the scan (on Fig. 3 the window is purposely out of focus to provide a slope calibration) and the integral A of the flux throughout the scan.

It can be shown that A depends only of the abscissa \underline{x}_0 of the true limb and practically not of the width of the spreading function. As, during a daily observational run, \underline{x}_0 varies because of guiding errors, variation of the refraction with zenith distance, and random image motion, a plot of \underline{x} against A is theoretically equivalent to a plot of \underline{x} against \underline{x}_0 . Fig. 4 is an example of such a plot. The non-symmetrical dispersion is conspicuous : it simply demonstrates the existence of the shift $\delta = \underline{x}_0 - \underline{x}$. The aim is to establish a calibration curve of δ against the maximum slope \underline{m} which is known for each point.

The first step is to draw a curve assumed to represent \underline{x}_0 against A, through the points known to have the highest values of \underline{m} . Then, the distance in ordinate of each point to the curve is a first approximation to the value of δ , referred to an arbitrary origin. Such values when plotted against the corresponding values of \underline{m} would lead to the correlation we are looking for. But now, to find the origin for \underline{x}_0 , and therefore the position of the true limb and the correct value of δ , one must extrapolate to large values of \underline{m} . Of course, this should be done on an inverse scale; we have chosen to number it conventionally in Full Width at Half Maximum, ϵ , of the gaussian spreading function which, applied to the HSRA limb, produces the slope \underline{m} . Where to extrapolate ? The theoretical FWHM of our objective is $0''25$, so that the maximum theoretical slope of the limb would correspond to about $0''30$. Fig. 5 shows the result for one day of observation under conditions we call "good", but not outstanding. For clarity each dot is the average of five points. A "very good day" shows a nice clustering of the points between $0''50$ and $0''35$.

The probable error on one scan can be estimated, at the moment, to $\pm 0''1$. But there are at least two reasons which substantially contribute to it and are to disappear soon. One is that, as said before, the curve \underline{x}_0 against A is a first approximation and should be improved by an iteration process which has not yet been applied here. The second and most obvious reason is that the sampling interval of the signal is, by now, as large as $0''8$, thus badly affecting the accuracy of the determination of \underline{x} ; this interval will be reduced, soon, to $0''2$. Therefore, we can expect that, in the final stage, the dispersion will fall well below, say, the pole-equator difference found by DICKE.

For the future of this experiment, an instrument which could logically be

called a heliometer is approaching completion, to be associated with the 50 cm refractor under our "turret-dome". The principle is to project the focal image (diameter about 60 mm) onto a Cer-Vit rod cut with sharp edges at both ends, slightly shorter than the solar diameter, and to scan both limbs simultaneously (Fig. 6). The diameter is the sum of the $(\underline{x} + \delta)$ quantities, as defined above for each limb, plus the length of the rod. The whole system rotates around the optical axis to explore all the solardiameters in succession. It is planned to have, in a next step, a permanent measurement of the focal length, in order to obtain at any time the angular diameter of the sun.

Now, we must mention an important by-product of these preliminary experiments, namely the oscillations of the value of the maximum gradient (YERLE, 1980). When plotting the values of \underline{m} for up to six hours of continuous observation, and computing the $\Delta I / I \Delta X$ values (in order to eliminate the variations of atmospheric transmission) residuals of the order of $\pm 2\%$ appear around a mean value which decreases from morning to afternoon. This trend is very likely due to the deterioration of the image quality while day-time is advancing. The difference between the values measured and an average curve gives the final residuals (Fig. 7), which could have two completely different origins, or both at once : either the time fluctuations of image quality, or solar effects.

The power-spectrum of these residuals (Fig. 8) shows an evident similarity with those obtained from high-sensitivity Doppler measurements of solar oscillations (ISAAK et al. 1979). It is not easy to imagine that local turbulence in the terrestrial atmosphere could present so definite frequencies in its fluctuations; but, as, unfortunately, it does exist, it should at least produce noise in the power spectrum.

As for the emergence of already known solar frequencies, an attractive explanation may be put forward, pending confirmation. It has been shown, above, that a change in temperature in the layers contributing to the formation of the limb changes the value of the maximum gradient; therefore, if spatial solar oscillations (e.g. at 3.3.m Hz) imply also temperature oscillations, they could appear in the gradient measurement.

Comparing the face value of $\pm 2\%$ for the fluctuation of the maximum gradient with the change produced by a temperature modification in region b_2 as it appears in Table I, one would conclude that it corresponds to a ΔT of about $\pm 70^\circ$. But in fact, the true amplitude of the gradient fluctuation must be corrected by a deconvolution using the spreading function at the moment of the scan, which can only increase the above value of the temperature change.

References

1. R.H. DICKE and H.M. GOLDENBERG, Phys. Rev. Letters. 18, 313 (1967)
2. H.A. HILL, R.T. STEBBINS and J.L. OLESON, Astrophys. J. 200, p. 472 and p.484 (1975)
3. H.A. HILL, private communication (1976)
4. H.A. HILL and T.P. CAUDELL, M.N.R.A.S., 186, 327 (1979)
5. J.B. ROGERSON, Ap. J., 130, 985 (1959)
6. H.A. HILL, R.D. ROSENWALD and T.P. CAUDELL, Ap. J. 225, 304 (1978)
7. J.E. VERNAZZA, E.H. AVRETT and R. LOESER, Center for Astrophysics, Cambridge Mass., Preprint Series n° 1308 (1980)
8. R. YERLE, 1980, Letter to the Editor submitted to A. and A.
9. G.R. ISAAK, A. CLAVERIE, C.P. Mc LEOD, H.B. van der RAAJ, 1979, Nature, 282, 591.

+
+
+

TABLE I

Layers n°	ΔT	\underline{x} arc sec.	Δx	$\Delta I/I \Delta X$ (°)
(a) 1 to 95	- 300	- 0.444	+ 0.018	6.77
	000	- 0.426	0.000	7.94
	+ 100	- 0.418	- 0.006	8.27
	+ 300	- 0.410	- 0.016	9.00
(b ₁) 1 to 30	+ 300	- 0.426	0.000	8.09
(b ₂) 31 to 65	+ 300	- 0.413	- 0.013	8.66
(b ₃) 66 to 95	+ 300	- 0.426	0.000	7.94
(c ₁) 95 to 1	0 to - 285	- 0.435	+ 0.009	7.51
(c ₂) 95 to 1	0 to + 285	- 0.420	- 0.006	8.36

(°) $\Delta I/I \Delta X$ expresses formally the relative change in brightness $\Delta I/I$ over a radial interval ΔX taken equal to 1"0, although the gradient is roughly constant over 0"2 only.

CAPTIONS

- Figure 1.- The HSRA model temperature vs height, and modifications introduced. In abscissæ, height in kilometers from the level $\tau_{5000} = 1$ at the center of the disk (positive for the inner photosphere, negative for the chromosphere). In ordinates, temperature in degrees K. Full line : normal HSRA model; -·-·-·-·- model a for constant ΔT from layers 1 to 95; models b₁, b₂, b₃ are shown for constant ΔT between layers 1 - 31, 31 - 66 and 66 - 95 respectively and zero elsewhere; ----- model c₂ with ΔT linear function of height, with zero at layer 95 (for the clarity, the ΔT on the figure are three times larger than those mentioned on Table I).
- Figure 2.- The solar limb computed from HSRA model; the origin in abscissæ is $\mu = 0$ for $\tau_{5000} = 1$; $\lambda = 5000 \text{ \AA}$; the intensity at the center of the disk is 32.8. Lower and left scales for the full line curve a; upper and right scales for the dashed curve b (where the location of portion a is indicated).
- Figure 3.- Oscilloscope tracings of the signal (top) and of its first derivative (bottom), showing the definitions of the abscissæ of point of maximum gradient on the true limb $L(x_o)$ and on the blurred limb $(x)(\delta$ is the shift), of the maximum gradient itself m, and of the integral flux A. For this preliminary experiment, the edges of the window limiting the scan are purposely blurred to provide a calibration of the gradient.
- Figure 4.- Observed correlation between the area (integral flux) measured and the abscissa of the point of maximum gradient. The slightly curved parabola shows the best fit among points corresponding to high values of m.
- Figure 5.- The correlation shift (arbitrary origin) vs FWHM (both in seconds of arc). The true origin for the shift should be determined by extrapolation to small values of FWHM (see text).
- Figure 6.- Left : the solar image, as seen looking to the sky. S_p and S_a are the solar images at perihelion and aphelion; R is the CERVIT rod; Rh_1 and Rh_2 are two rhombohedra; S_ℓ and S_r are the portions of the limb as seen through the rhombohedra. Right : the profile of a complete scan, on left limb ℓ , calibration beam b, (drawn from the center of the disk) and right limb r , with scales in arc and time seconds.

Figure 7.- Residuals of $\Delta I/I\Delta X$ on Sept. 11, 1979, in percent of the average value. A periodicity of about two and half hours is visible but has to be confirmed.

Figure 8.- Power spectra : top, of the maximum gradient on the limb, on Sept. 11, 1979, expressed in $(\text{arc sec}^{-1})^2 \text{mHz}^{-1}$ (YERLE, 1980); middle and bottom, of integrated radial velocity, measured simultaneously at Izaña and Pic du Midi on Aug. 8. 1978, expressed in $(\text{ms}^{-1})^2 \text{m Hz}^{-1}$ (ISAAK et al., 1979).

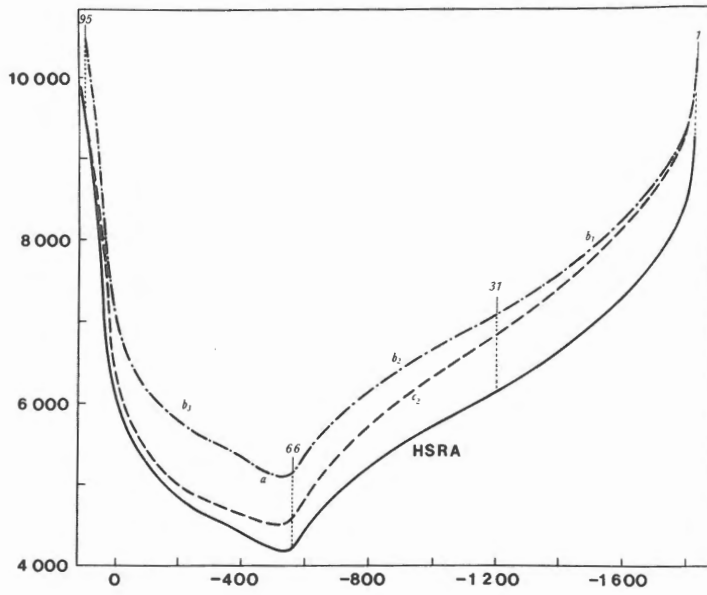


Figure 1.

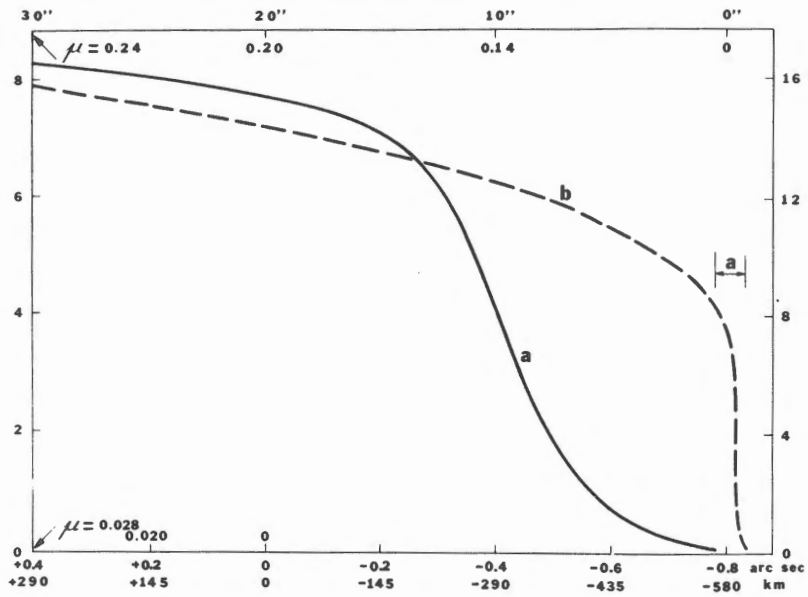


Figure 2.

Figure 3.

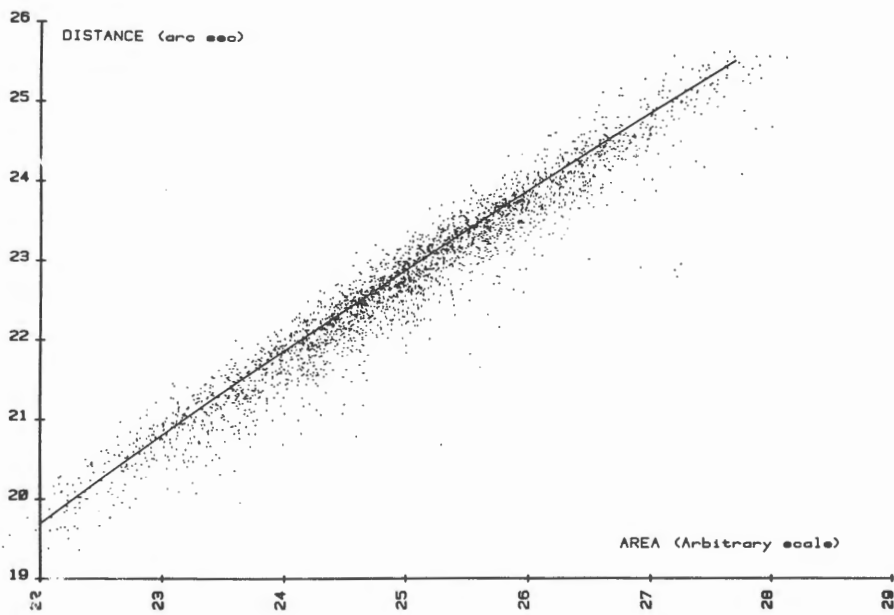
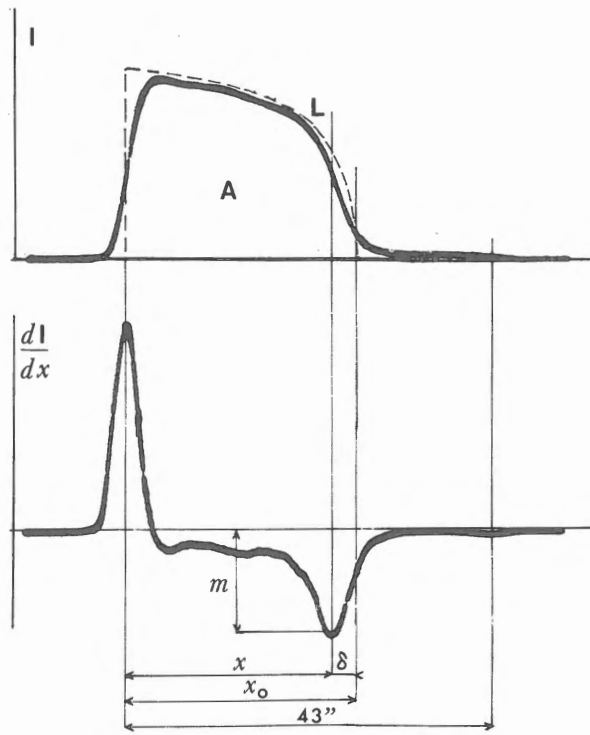


Figure 4.

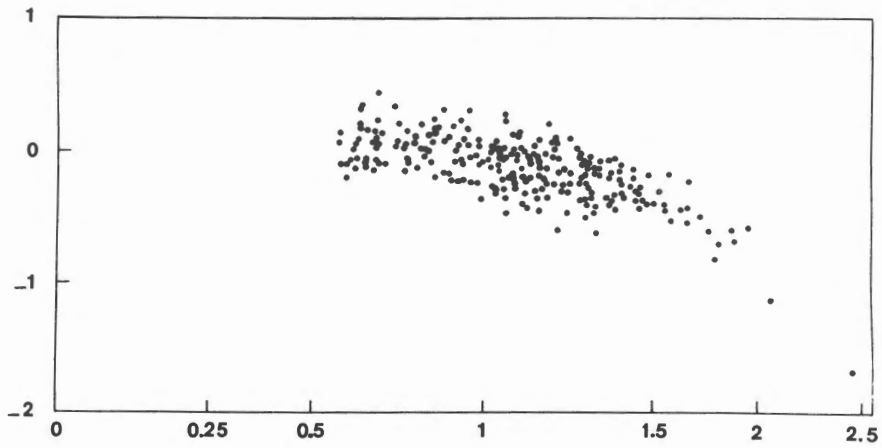


Figure 5.

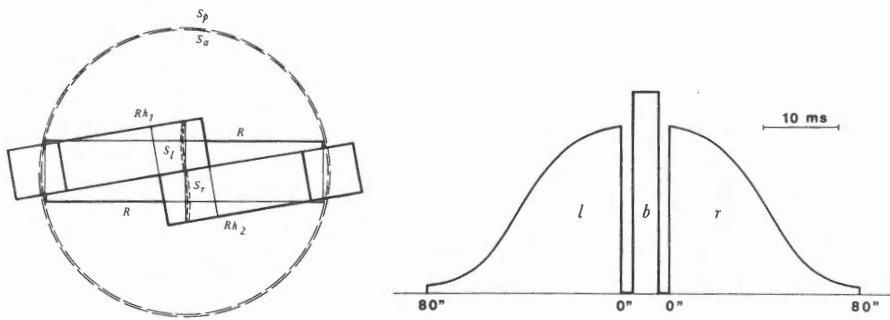


Figure 6.

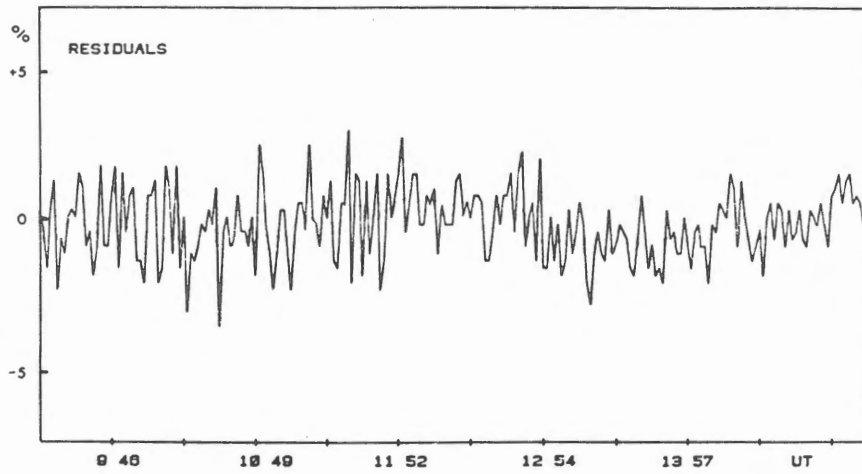


Figure 7.

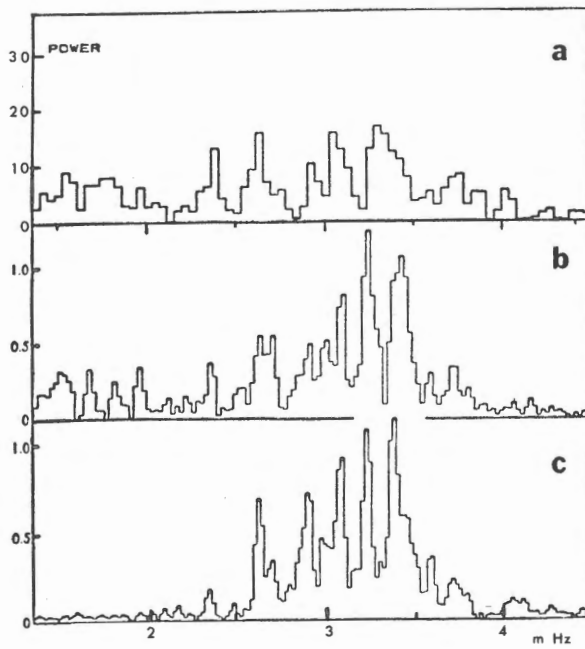


Figure 8.